



## Comprehensive investigation of Ge–Si bonded interfaces using oxygen radical activation

Ki Yeol Byun, Pete Fleming, Nick Bennett, Farzan Gity, Patrick McNally, Michael Morris, Isabelle Ferain, and Cindy Colinge

Citation: *Journal of Applied Physics* **109**, 123529 (2011); doi: 10.1063/1.3601355

View online: <http://dx.doi.org/10.1063/1.3601355>

View Table of Contents: <http://scitation.aip.org/content/aip/journal/jap/109/12?ver=pdfcov>

Published by the [AIP Publishing](#)

---

### Articles you may be interested in

[Scanning x-ray microtopographs of misfit dislocations at SiGe/Si interfaces](#)

*Appl. Phys. Lett.* **79**, 2363 (2001); 10.1063/1.1408601

[On the use of total reflection x-ray topography for the observation of misfit dislocation strain at the surface of a Si/Ge–Si heterostructure](#)

*Appl. Phys. Lett.* **77**, 1644 (2000); 10.1063/1.1308269

[Controlling threading dislocation densities in Ge on Si using graded SiGe layers and chemical-mechanical polishing](#)

*Appl. Phys. Lett.* **72**, 1718 (1998); 10.1063/1.121162

[Effect of the surface upon misfit dislocation velocities during the growth and annealing of SiGe/Si \(001\) heterostructures](#)

*J. Appl. Phys.* **83**, 1931 (1998); 10.1063/1.366984

[Novel dislocation structure and surface morphology effects in relaxed Ge/Si-Ge\(graded\)/Si structures](#)

*J. Appl. Phys.* **81**, 3108 (1997); 10.1063/1.364345

---



# Comprehensive investigation of Ge–Si bonded interfaces using oxygen radical activation

Ki Yeol Byun,<sup>1</sup> Pete Fleming,<sup>2</sup> Nick Bennett,<sup>3</sup> Farzan Gity,<sup>1</sup> Patrick McNally,<sup>3</sup> Michael Morris,<sup>1,4</sup> Isabelle Ferain,<sup>1</sup> and Cindy Colinge<sup>1</sup>

<sup>1</sup>Tyndall National Institute, University College Cork, Dyke Parade, Cork, Ireland

<sup>2</sup>Environmental Research Institute, University College Cork, Cork, Ireland

<sup>3</sup>School of Electronic Engineering, Dublin City University, Dublin, Ireland

<sup>4</sup>Department of Chemistry, University College Cork, Cork, Ireland

(Received 18 January 2011; accepted 16 May 2011; published online 27 June 2011)

In this work, we investigate the directly bonded germanium-silicon interfaces to facilitate the development of high quality germanium silicon hetero integration at the wafer scale. X-ray photoelectron spectroscopy data is presented which provides the chemical composition of the germanium surfaces as a function of the hydrophilic bonding reaction at the interface. The bonding process induced long range deformation is detected by synchrotron x-ray topography. The hetero-interface is characterized by measuring forward and reverse current, and by high resolution transmission electron microscopy. © 2011 American Institute of Physics. [doi:10.1063/1.3601355]

## I. INTRODUCTION

Germanium (Ge) has been considered as a promising candidate to overcome the limitation of silicon (Si) for next generation complementary metal-oxide-semiconductor (CMOS) devices and optoelectronics. The higher mobility enhances drift current resulting in higher source injection velocity and higher drive current.<sup>1</sup> For optoelectronics Ge can absorb light in the infrared region, which makes it attractive for integration of monolithic optical components with Si leading to photodetection at telecommunication wavelengths (from 1.31  $\mu\text{m}$  to 1.55  $\mu\text{m}$ ).<sup>2</sup> Furthermore, the Ge based optical communication circuits can be monolithically integrated with Si transistor technology.

Epitaxial crystal growth is a method for integration of hetero-structures between dissimilar materials. However, conventional epitaxial Ge growth on Si requires careful processing to minimize the impact of the dislocations caused by the lattice mismatch and large thermal expansion coefficient difference between Ge and Si.<sup>3</sup> Such defects can create generation centers that contribute to the leakage current in minority carrier devices.

Low temperature direct wafer bonding is a simple and easy alternative method for forming hetero-structures without these limitations at the wafer scale. Recently Ge to Si direct bonding has been studied for use in high-performance avalanche photodiode (APD).<sup>4</sup> It is important to clarify the quality of the hetero-interface and performance of devices fabricated using bonded Ge–Si hetero-junction. Recently several reports have discussed direct observations using transmission electron microscopy (TEM) of the Ge–Si hetero-interface formed by direct wafer bonding.<sup>5,6</sup>

In our previous report, a low temperature radical activated Ge–Si wafer bonding method was developed, to achieve good bond strength with a low thermal budget and as a result mitigates defect generation common in epitaxial growth.<sup>7</sup> In this paper, we have investigated the transition of

the chemical states of Ge as a function of the hydrophilic reaction at the Ge–Si interface formed by wafer bonding and thermal annealing at low temperature (200 and 300 °C) using x-ray photoelectron spectroscopy (XPS). Further, the deformation induced by strain at the bonded hetero-interface was detected by synchrotron x-ray topography. Hetero-interface conductivity was characterized by measuring the forward and reverse current. The observation of the hetero-junction was supported by high resolution (HR) transmission electron microscopy (TEM).

## II. EXPERIMENTAL

In this experiment, 4-inch (100)-oriented p-type blanket Ge wafers (Ga doped, resistivity = 0.016  $\Omega\text{ cm}$ , 450  $\mu\text{m}$ ) and (100)-oriented n-type Czochralski blanket Si wafers (P doped, resistivity = 2–4  $\Omega\text{ cm}$ , 530  $\mu\text{m}$ ) were selected for direct wafer bonding. Prior to bonding, the Ge and Si wafers were cleaned in a dilute ammonium hydroxide–hydrofluoric acid–water mixture with and without ozone for Si and Ge, respectively, in a spray acid tool (SAT) referred to as an equivalent Standard Clean 1 (SC1). Wafers were then loaded into an Applied Microengineering Limited (AML) AW04 aligner bonder and vacuum was applied. Two different conditions were used prior to bonding. In the first experiment (reference sample), Si and Ge wafers were loaded into the AML bonder and the chamber was pumped down to  $10^{-5}$  mbar. The wafer pair was then bonded *in situ*. After bonding, a force 1 kN was applied for 5 min at  $10^{-5}$  mbar. In a second experiment, the Si and Ge wafers were loaded into AML and the wafers were then exposed for 10 min to oxygen free radicals generated by a remote plasma ring. The chamber pressure during remote plasma exposure was 1 mbar at 100 W.<sup>8</sup> After exposure, the Si and Ge wafers were bonded *in situ* under a force of 1 kN applied for 5 min at a chamber pressure of  $10^{-5}$  mbar. Both sets of wafers were then annealed *in situ* at 100 °C for 1 h with a 500 N force. This operation was

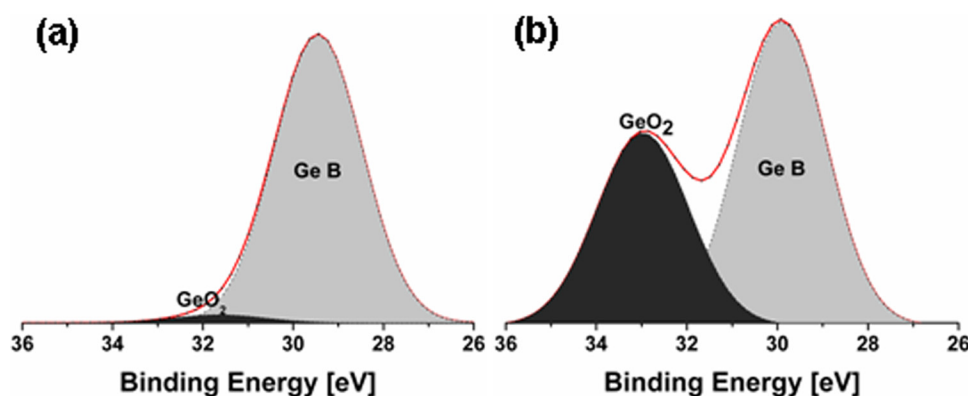


FIG. 1. (Color online) XPS spectrum of the Ge 3d core level of de-bonded Ge surface at post-bonding and post two step annealing (Takeoff angle =  $0^\circ$ ): (a) cleaned in an SC1-equivalent solution (reference sample) and (b) for sample with SC1-equivalent clean followed by  $O_2$  radical 10 min exposure prior to bonding. Each contribution to the shape is single out and marked as Ge B (Ge bulk peak) and  $GeO_2$ .

followed by an *ex-situ* anneal at  $200^\circ\text{C}$  for 24 h in order to enhance the bond strength. The two sets of bonded wafers were then annealed again at  $300^\circ\text{C}$  for 24 h. The temperature ramp rate was set to  $0.5^\circ\text{C}/\text{min}$  in the two step annealing process.

The transition of chemical components on the Ge surfaces (with and without oxygen radical exposure) was investigated by means of *ex-situ* XPS.<sup>9</sup> The XPS was used to measure the reference sample and free radical exposed sample to determine the Ge surface components after the two step anneal. XPS analysis was performed by using 1486.6 eV x-rays generated from an Al  $K\alpha$  source, which illuminated the Ge surfaces of the samples placed into a ultrahigh vacuum immediately after de-bonding the Ge–Si bonded pairs.

To investigate deformation induced by strain at the bonded Ge–Si interface, bonded pieces of the same two samples were measured by synchrotron x-ray topography. The topographs were taken at ANKA, Karlsruhe, Germany using the continuous radiation spectrum emitted by a bending magnet source in the storage ring. The positron ring has a particle momentum of 2.5 GeV, white beam energy range of 1.5–33 keV and a beam current of 100–180 mA. The topographs were recorded either on a high-resolution Slavich holographic film (grain size  $\sim 0.04\ \mu\text{m}$ )—set 85 mm from the sample in back-reflection geometry—or by CCD camera—set 120 mm behind the sample in transmission geometry, respectively. A square beam, incident perpendicular to the sample surface and with spot size between  $6\ \text{mm} \times 6\ \text{mm}$  and  $2\ \text{mm} \times 2\ \text{mm}$ , was employed for large area measurements. Subsequently, LAUEPT software was used to index the individual topographs. For the reflections captured on film, individual topographs were magnified using an optical microscope allowing the features to be observed and analyzed. Large area back reflection topography (LABRT) was carried out on these samples.

To characterize electrical properties of the bonded hetero-interface, p-type Ge wafers (Ga doped, resistivity =  $0.02\ \Omega\ \text{cm}$ , 225  $\mu\text{m}$ ) were bonded directly to highly doped n-type Si wafer (P doped, resistivity =  $0.001\ \Omega\ \text{cm}$ , 530  $\mu\text{m}$ ) using 10 min oxygen radical exposure and annealed at  $200^\circ\text{C}$  for 24 h and additionally  $300^\circ\text{C}$  for 24 h. Prior to surface activation, all wafers were cleaned in a SC1-equivalent solution.

Test mesa structure was fabricated by a semi-dicing technique.<sup>10</sup> The method used a semi-dicing technique to saw entirely through the bonded interface, but still left sufficient thickness of the Si–Ge wafer sandwich for easy handling. The edges of the sawed p–n mesas were chemically etched using 10:1 HF solution (20 s) followed by a DI rinse to remove saw damage prior to testing. The bonded Ge–Si hetero-junction was characterized by measuring the forward and reverse current with Au metal contacts on Ge and Si wafers. Further, the hetero-interface was characterized by HR-TEM.

### III. RESULTS AND DISCUSSION

Free radical exposure prior to direct wafer bonding can generate a thin  $GeO_2$  film on Ge surface as reported in our previous report.<sup>7</sup> In that study, the hydrophilic bonding reactions at the Ge–Si interface have been described using Eqs. (1) and (2):

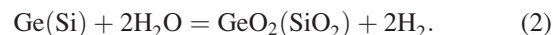


Figure 1 shows the XPS spectrum of the Ge 3d core level for the Ge surface. It is shown at post bonding and annealing condition for the two Ge–Si samples which include a reference sample which was not activated using oxygen free radicals prior to bonding (Fig. 1(a)) and a sample which was exposed to oxygen free radicals prior to bonding (Fig. 1(b)). After Shirley background subtraction, curve-fitting of the spectra was performed to reveal the changes in the surface chemistry occurring at the interface by applying two contributions with Gaussian–Lorentzian line shapes; the elemental peak (Ge B) at a binding energy (BE) = 29.5 eV and the oxidized state component ( $GeO_2$ ) at a binding energy (BE) = 32.4 eV.<sup>11</sup> Prior to bonding, radical exposed Ge surface showed higher values of O/Ge ratio, which was due to a thicker  $GeO_2$  film compared to the reference Ge sample.<sup>7</sup> In Fig. 1(a), it is shown that the passive film, formed on hydrophilic cleaning, appears to prevent bulk oxidation after the bonded wafers are annealed at 200 and  $300^\circ\text{C}$  for 24 h. On the contrary, an oxygen radical exposed passive film allows for bulk oxidation via diffusion of a reactive  $H_2O$  species by

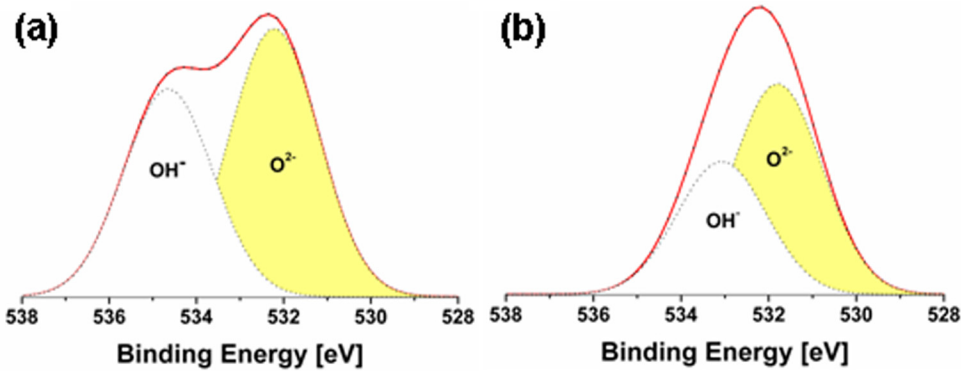


FIG. 2. (Color online) XPS spectrum of the O 1s core level of de-bonded Ge surface at post-bonding and post two step annealing (Takeoff angle = 0°): (a) cleaned in an SC1-equivalent solution and (b) cleaned in SC1-equivalent followed by O<sub>2</sub> radical 10 min exposure.

means of hydrophilic reaction (Eq. (2)) which then creates a thicker GeO<sub>2</sub> film (Fig. 1(b)).

O 1s spectra provide information on the nature of these surfaces.<sup>12</sup> In all cases, O 1s spectra could only be suitably fitted using two oxygen environments as shown in Fig. 2 for the samples described in Fig. 1. We assign these states to oxide (O<sup>2-</sup> in GeO<sub>2</sub>) at ~531.5 eV and OH<sup>-</sup> species at ~532.7 eV. In Ref. 7 it was clear that both cleaned and oxygen radical exposed Ge surface are largely hydrolyzed and the spectra are dominated by the hydroxide component prior to bonding. This is consistent with a surface preparation to ensure hydrophilic bonding. After bonding and anneal (Fig. 2 (a)) a greater contribution of O<sup>2-</sup> can be observed. This is wholly expected from Eq. (1) where bonding is a condensation of the hydrolyzed surface. In Fig. 2(b) the data shows an even further increase in the O<sup>2-</sup> component for the oxygen free-radical exposed sample. This is as expected because of the increased oxygen at the Ge and Si surfaces which results in a bulk oxidation process via sub-surface diffusion as shown from data in Fig. 1(b). Further discussion of the binding energy of OH<sup>-</sup> species in Fig. 2(a) is needed. The apparent binding energy of the OH<sup>-</sup> feature has been shifted to around 535 eV. There are two possible reasons for this. First, the surface may contain trapped water, which results in a feature around this binding energy<sup>13</sup> or there are localized regions where surface oxidation results in film thicknesses which lead to localized surface charging and shifting of these features. This XPS data after bonding and

anneal corresponds to our previous result that radical activated samples generate a relatively thicker oxide interfaces which results in minimal intrinsic voids due to enhancement of by-product diffusion.<sup>7</sup>

Among non-destructive methods to judge the quality of bonding, x-ray topography is probably the most sensitive technique.<sup>14</sup> Similar to x-ray diffraction, synchrotron x-ray topography is a non-destructive method that is ideal for studying high quality crystalline materials. It is able to image the defects and strain fields distributed within the crystals with selectable surface profile depths ranging from 10 to 1 mm. To explore the deformation at bonded interfaces as a function of the activation technique, LABRT analyses were carried out on all bonded Ge-Si samples. Figure 3(a) shows a -1 -1 8 large area back reflection topograph for the reference sample. The key features to note are the roughly circular “bubbles” dispersed across the topograph; these are more prevalent in the bottom left corner. These almost certainly represent the long range strain fields associated with voids at the Ge/Si interface, which is evidence of some degree of delamination.<sup>15</sup> Although the x-ray beam penetrates significantly shallower than the depth of the interface we are able to image the bubbles as the strain fields transpire across hundreds of microns in thickness. In contrast to the topograph for the reference sample in Fig. 3(a), Fig. 3(b) shows evidence of very few bubbles contained at the Ge-Si interface for oxygen radical exposed sample (dark spots are most likely due to dirt on the film). In this case there is some evidence of white lines running across the topographs. A more quantitative comparative analysis is shown in Table. I. The details were extracted using manual visual inspection of the magnified topographs. For the reference samples, the generated “bubbles” result in formation of a strain field close to delaminated region. For oxygen radical exposure, the increased GeO<sub>2</sub> by means of hydrophilic reaction induces

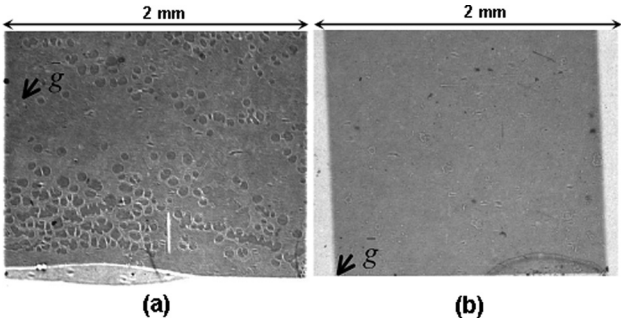


FIG. 3. Large area back reflection topographs taken with -1 -1 8 reflection of Ge-Si bonded samples after two step anneal: (a) cleaned in SC1-equivalent solution, and (b) followed by O<sub>2</sub> radical 10 min exposure.

TABLE I. Details of “bubble” observed in LABRT.

Sample	Density (cm <sup>-2</sup> )	Typical size (um)	Bubble shape
SC1 cleaned	5000	20–60	round type
SC1 + O <sub>2</sub> radical	300	20–50	variable



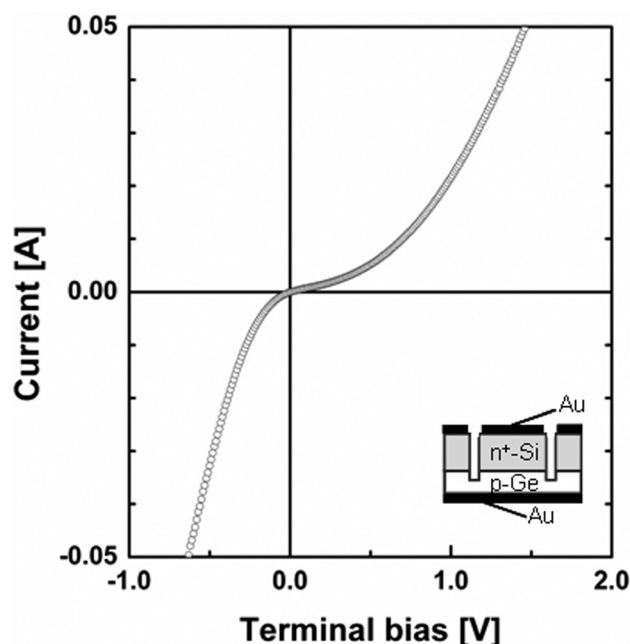


FIG. 4. Current-voltage characteristics of a  $p$ - $n$  junction fabricated by oxygen radical activated wafer bonding.

less strain field at the bonded interface, which results in less “bubbles.” Further large area topography investigation using bonded double side polished Si and Ge wafers will be reported. Double side polished bonded wafers allow for better imaging including 3D section scans.

The current-voltage ( $I$ - $V$ ) characteristics of the bonded sample which was activated with oxygen has been measured using the  $p$ -type Ge/ $n^+$ -type Si diode structure. High doping from the Si sides ensures a high density of mobile carriers for enhanced charge transfer.  $I$ - $V$  characterization was performed using Agilent B1500 semiconductor parameter analyzer and the result is shown in Fig. 4. for a  $5 \times 5$  mm<sup>2</sup> diodes. Recently the  $I$ - $V$  behavior at the Si-Ge hetero-interface has been reported using 200 nm  $n^+$ -Si ( $4 \times 10^{20}$ /cm<sup>3</sup>) bonded to a  $p^+$ -Ge ( $1 \times 10^{20}$ /cm<sup>3</sup>) wafer, which is similar to

the doping profile of our device structure.<sup>16</sup> As comparison, our measured current flow through bonded the hetero-junction appears to be similar to plots shown in Ref. 16. The depletion layer width for  $p$ -type Ge/ $n^+$ -type Si hetero-junction is considerably narrower than those of conventional  $p$ - $n$  junction, which enables the carriers to tunnel across the interface. Hence the resistance of our bonded hetero-junction is significantly low,  $< 5.0 \Omega \text{ cm}^2$ , in the negative terminal bias (forward region). However, at higher positive terminal bias (reverse region), the conduction has become limited by the series resistance of bulk substrate.

Figure 5 shows HR-TEM micrograph of the bonded  $p$ -type Ge/ $n^+$ -type Si hetero-interface. The interfacial region appears to be amorphous and approximately 2 nm thick. Based on XPS analysis as shown in Figs. 1 and 2, we conclude that the bonded Si/Ge interface is a thin amorphous oxide created by the hydrophilic reaction. It is known that hydrophobic bonding produces less oxide at the interface which will results in higher conductivity cross the bonded interface.<sup>16</sup> However, the 2 nm amorphous interface is small enough to allow conductivity by means of tunneling. Consequently our hydrophilic direct wafer bonding using oxygen radical exposure is feasible for fabrication of a Ge-Si  $p$ - $n$  junction.

#### IV. CONCLUSION

The reaction product at Ge-Si bonded interfaces has been investigated. It has been demonstrated that oxygen radical exposure prior to bonding can enhance a conversion of the bulk Ge to GeO<sub>2</sub> by means of an interfacial hydrophilic reaction. The generated thin film contributes to a reduction of process induced long range deformation. Electrical characterization of  $p$ - $n$  junctions formed by oxygen radical activated bonding indicates high conductivity at across the bonded Ge-Si interface. This conclusion is useful for high quality hetero-structure integration of thermally mismatched materials such as those used for photonic devices. Currently we are working on achieving even higher conductivity by appropriate surface preparation prior to radical exposure and optimization of the thermal treatment.

#### ACKNOWLEDGMENTS

This work was supported by the Science Foundation Ireland Grant No. 07/IN/I937: Low Temperature Wafer Bonding for Heterogeneous Integration.

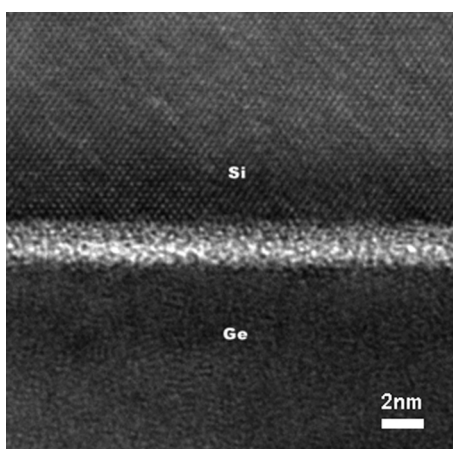


FIG. 5. HR-TEM micrographs of the bonded  $n^+$ -Si/ $p$ -Ge interface after two step anneal: cleaned in an SC1-equivalent solution followed by O<sub>2</sub> radical 10 min exposure.

<sup>1</sup>K. Krishnamohan, C. Jungemann, D. Kim, E. Ungersboeck, S. Selberherr, A. Pham, B. Meinerzhagen, P. Wong, Y. Nishi, and K. Saraswat, *Microelectron. Eng.* **84**, 2063 (2007).

<sup>2</sup>Z. Huang, N. Kong, X. Guo, M. Liu, N. Duan, A. Beck, S. Banerjee, and J. Campbell, *IEEE J. Sel. Top. Quantum Electron.* **12**, 1450 (2006).

<sup>3</sup>J. Michel, J. Liu, and L. Kimerling, *Nat. Photon.* **4**, 527 (2010).

<sup>4</sup>L. Chen, P. Dong, and M. Lipson, *Opt. Express* **16**, 11513 (2008).

<sup>5</sup>M. Kim, R. Carpenter, *J. Electron. Mater.* **32**, 849 (2003).

<sup>6</sup>H. Kanbe, M. Hirose, T. Ito, and M. Taniwaki, *J. Electron. Mater.* **39**, 1248 (2010).

- <sup>7</sup>K. Byun, I. Ferain, P. Fleming, M. Morris, M. Goorsky, and C. Colinge, *Appl. Phys. Lett.* **96**, 102110 (2010).
- <sup>8</sup>K. Byun, I. Ferain, and C. Colinge, *J. Electrochem. Soc.* **157**, H109 (2010).
- <sup>9</sup>K. Nakayama, K. Tanabe, and H. Atwater, *J. Appl. Phys.* **103**, 094503 (2008).
- <sup>10</sup>K. Hobart, M. Twigg, F. Kub, and C. Desmond, *Appl Phys Lett.* **72**, 1095 (1998).
- <sup>11</sup>N. Tabet, M. Faiz, N. Hamdan, and Z. Hussain, *Surf. Sci.* **523**, 68 (2003).
- <sup>12</sup>J. Oh, and J. Campbell, *J. Electron. Mater.* **33**, 364 (2004).
- <sup>13</sup>T. Teng, W. Lee, Y. Chang, J. Jiang, T. Wang, and W. Hung, *J. Phys. Chem. C* **114**, 1019 (2010).
- <sup>14</sup>G. Horn, Y. Chu, Y. Zhong, T. Mackin, J. Lesniak, and D. Reiniger, *J. Electrochem. Soc.* **155**, H36 (2008).
- <sup>15</sup>T. Argunova, J. Yi, J. Jung, J. Je, L. Sorokin, M. Gutkin, E. Belyakova, L. Kostina, A. Zabrodskii, and N. Abrosimov, *Phys. Status Solidi A* **204**, 2669 (2007).
- <sup>16</sup>A. Kiefer, D. Paskiewicz, A. Clausen, W. Buchwald, R. Soref, and M. Lagally, *ACS Nano* **5**, 1179 (2011).